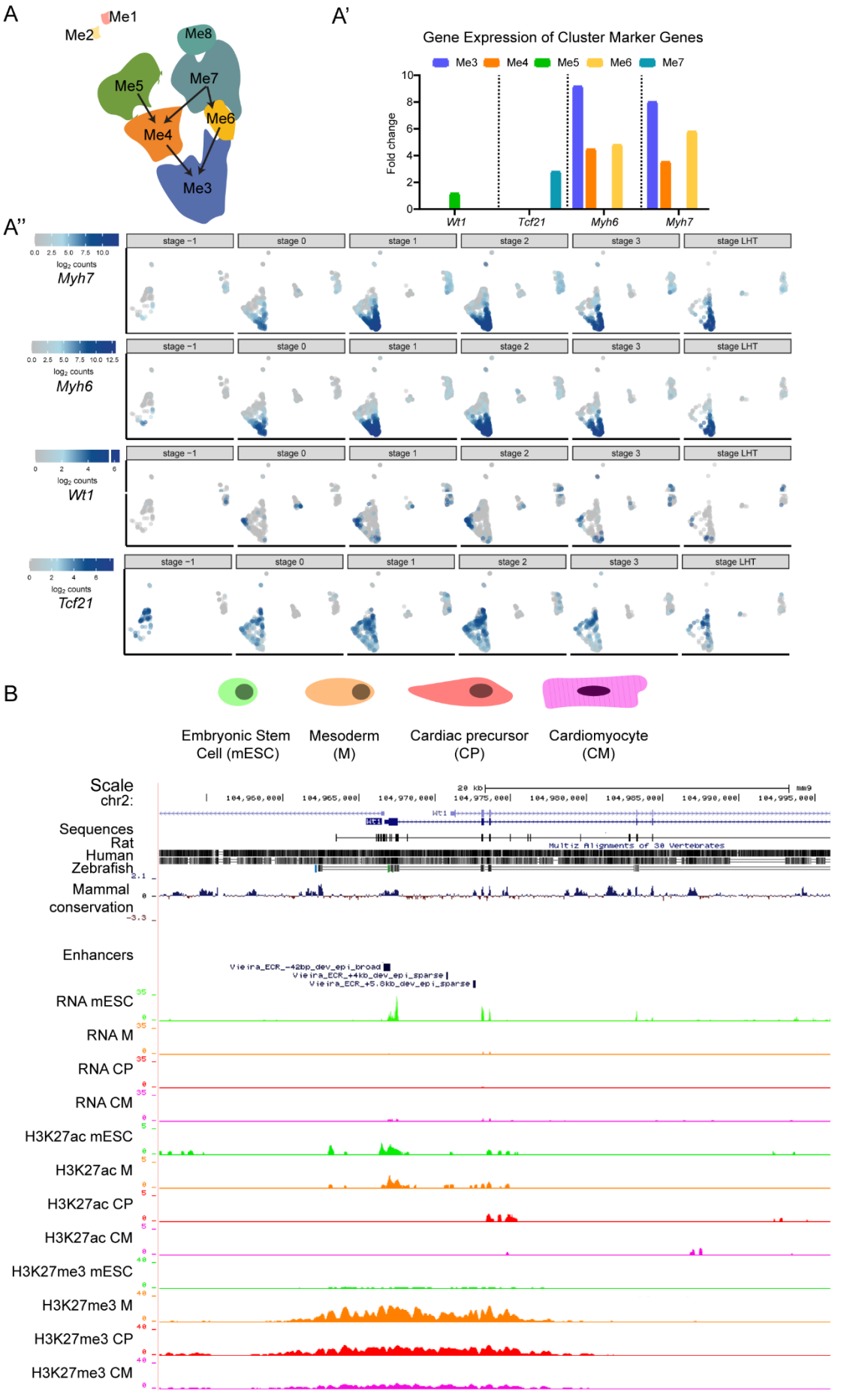

Fig. S1.

Fig. S1. Transcriptional and histone modification signatures of *Wt1* through cardiac developmental and differentiation stages *in vivo* and *in vitro* across mouse heart and embryonic stem cells.

(A-A") Re-analysis of published single cell RNAseq data from mouse embryos (Tyser et al., 2021). (A) Schematic representation of the developmental trajectories of mesothelial cardiac cell populations (Tyser et al., 2021). (A') Fold change in the expression levels of cluster marker genes: *Wt1*, *Tcf21*, *Mhy6* and *Myh7*. (A") Spatio-temporal gene expression of genes shown in A' in different developmental cardiac cell trajectories. (B) UCSC browser gene tracks depicting the *Wt1* locus and associated transcriptomic and epigenomic signatures in mouse embryonic stem cells (mESC), mesodermal progenitors (M), cardiac precursors (CP) and cardiomyocytes (CM), as published previously (Wamstad et al., 2012). Tracks of activating H3K27ac and repressive H3K27me3 marks are shown and co-localizing elements with previously validated epicardial enhancer activities 4kb and 5.8kb downstream of the *Wt1* transcriptional start site (TSS) are indicated (Vieira et al., 2017). Shown tracks represent the sum of the tracks for the different samples, for each type of cell. Mammal conservation is illustrated by the Placental Mammal base wise conservation track by PhyloP.

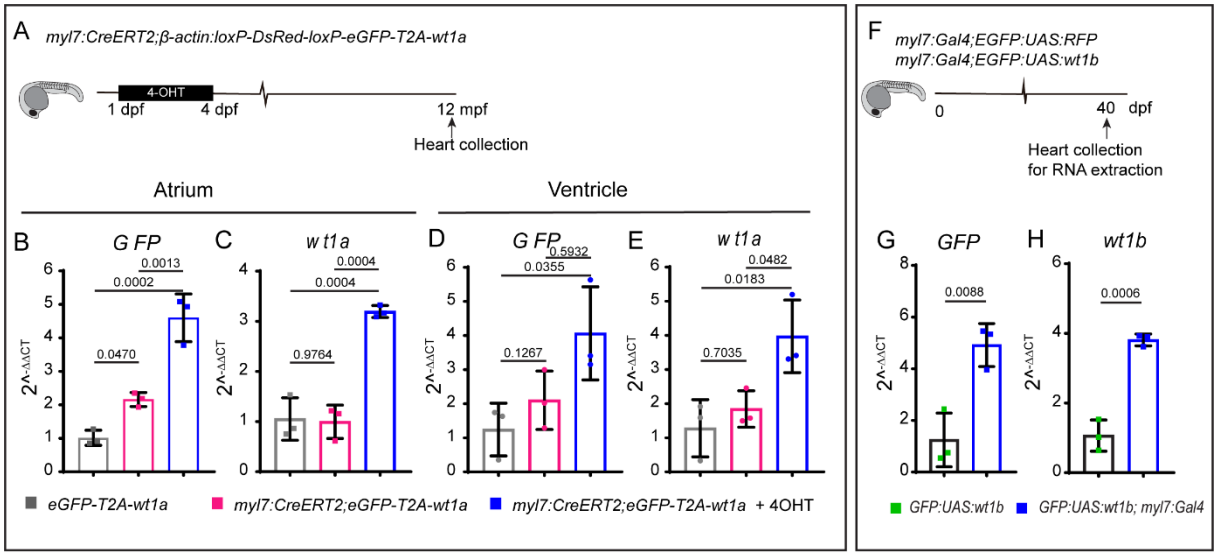

Fig. S2

Fig. S2. Validation of the *wt1a* and *wt1b* overexpression lines.

(A) Schematic representation of the time points during which 4-Hydroxytamoxifen (4-OHT) was administered to *myl7:CreERT2;β-actin:loxP-DsRed-loxP-eGFP-T2A-wt1a* fish (in short *myl7:CreERT2,eGFP-T2A-wt1a*) and tissue collection.

(B-E) qRT-PCR for *GFP* (B,D) and *wt1a* (C,E) on adult heart cDNA from *myl7:CreERT2, eGFP-T2A-wt1a* with and without 4-OHT. qRT-PCR was performed on cDNA obtained from the atrium (B,C) and (D,E) ventricles. Points represent biological replicates, 3 for each group. Statistical significance was calculated using one-way ANOVA. Shown are means ±SD.

(F) Schematic representation of lines used and the time at which RNA was extracted.

(G-H) qRT-PCR for *eGFP* (G) and *wt1b* (H) in *eGFP:UAS:wt1b* and *myl7:Gal4;eGFP:UAS:wt1b* hearts at 40 days post fertilization (dpf). The points represent biological replicates. Statistical significance was calculated with an unpaired t-test. Shown are also means ±SD.

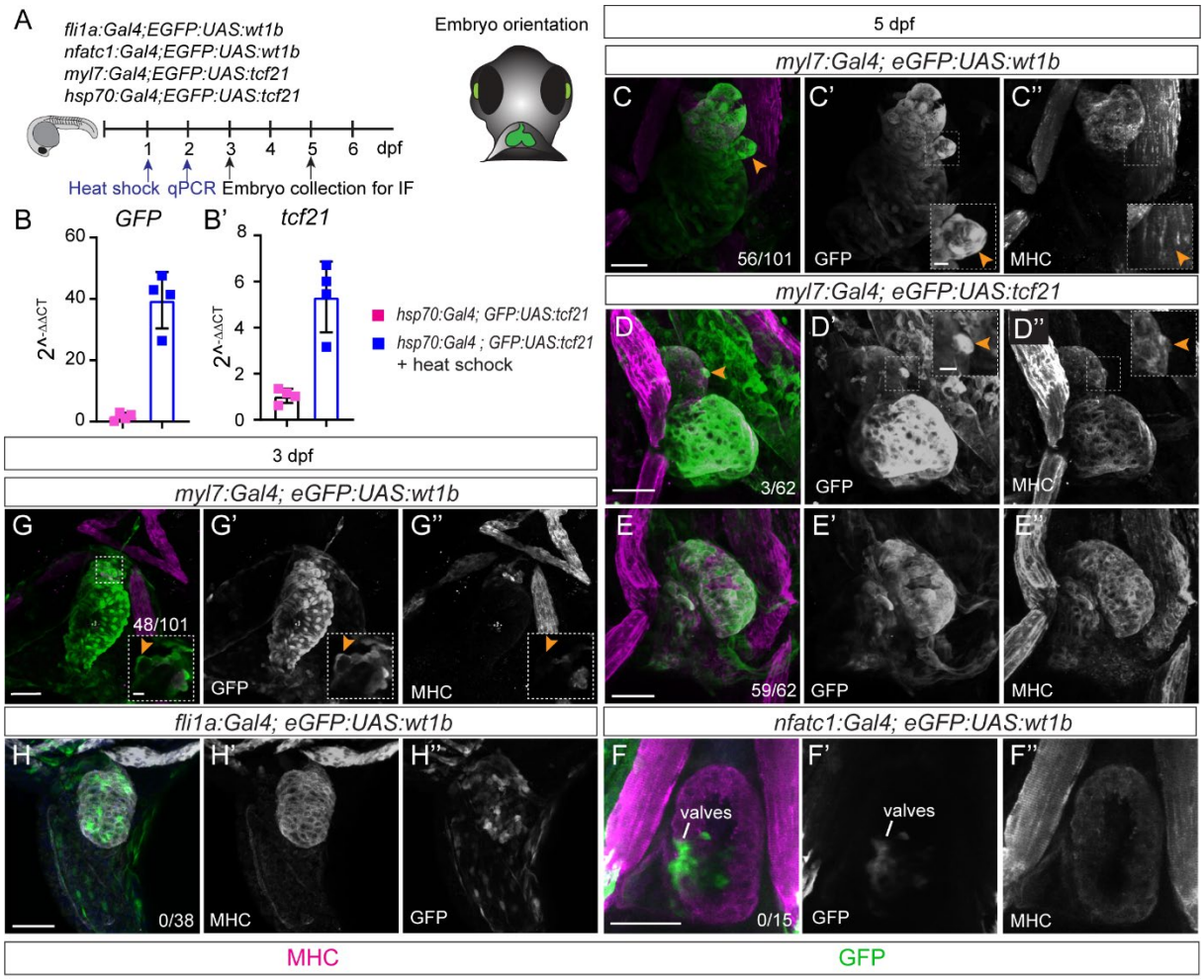

Fig. S3

Fig. S3. Overexpression of *tcf21* transcription factor in cardiomyocytes and *wt1b* in non-cardiomyocytes does not affect heart development.

(A) Schematic representation of the lines used and embryo orientation for imaging. (B-B') qRT-PCR for GFP (B) and tcf21 (B') on 48 hours post-fertilization (hpf) zebrafish embryos. cDNA from *hsp70:Gal4;eGFP:UAS:tcf21* with and without heat-shock. Points represent biological replicates, 3 for each group. Statistical significance was calculated using unpaired t-test with Welch's correction. Shown are means ±SD. (C-H") Immunofluorescence against GFP and myosin heavy chain (MHC) on *myl7:Gal4;eGFP:UAS:wt1b*, *myl7:Gal4;eGFP:UAS:tcf21, fli1a:Gal4;eGFP:UAS:wt1b* and *nfatc1:Gal4;eGFP:UAS:wt1b* zebrafish embryos, at 3 or 5 days post fertilization (dpf). (C-C") Shown are 3D projections of a *myl7:Gal4;eGFP:UAS:wt1b* heart in a ventral view, at 5 dpf. (C'-C") show single channels for GFP and MHC. The box highlights a zoomed region in the heart where a cluster of delaminating cells can be seen. (C") Note the absence of MHC in the delaminated cells. (D-E") Shown are 3D

projections of a *myl7:Gal4;eGFP:UAS:tcf21* heart in a ventral view, at 5 dpf. (D-D”) show single channels for GFP and MHC. The box highlights a zoomed region in the heart with one cell delaminating. Note in D” that the delaminating cell preserved MHC expression. (F-F”) Shown are maximum intensity projections of 5 stacks with a distance of 1.5 µm between two consecutive optical sections of the heart region of a *nfatc1:Gal4;eGFP:UAS:wt1b* heart in a ventral view, at 5 dpf. GFP expression is observed in the valve region. The number of embryos with delaminating cells is indicated in the panels. Green, GFP; magenta, MHC. Scale bar 50 µm and 10 µm, in the zoom boxes. at, atrium; v, ventricle.

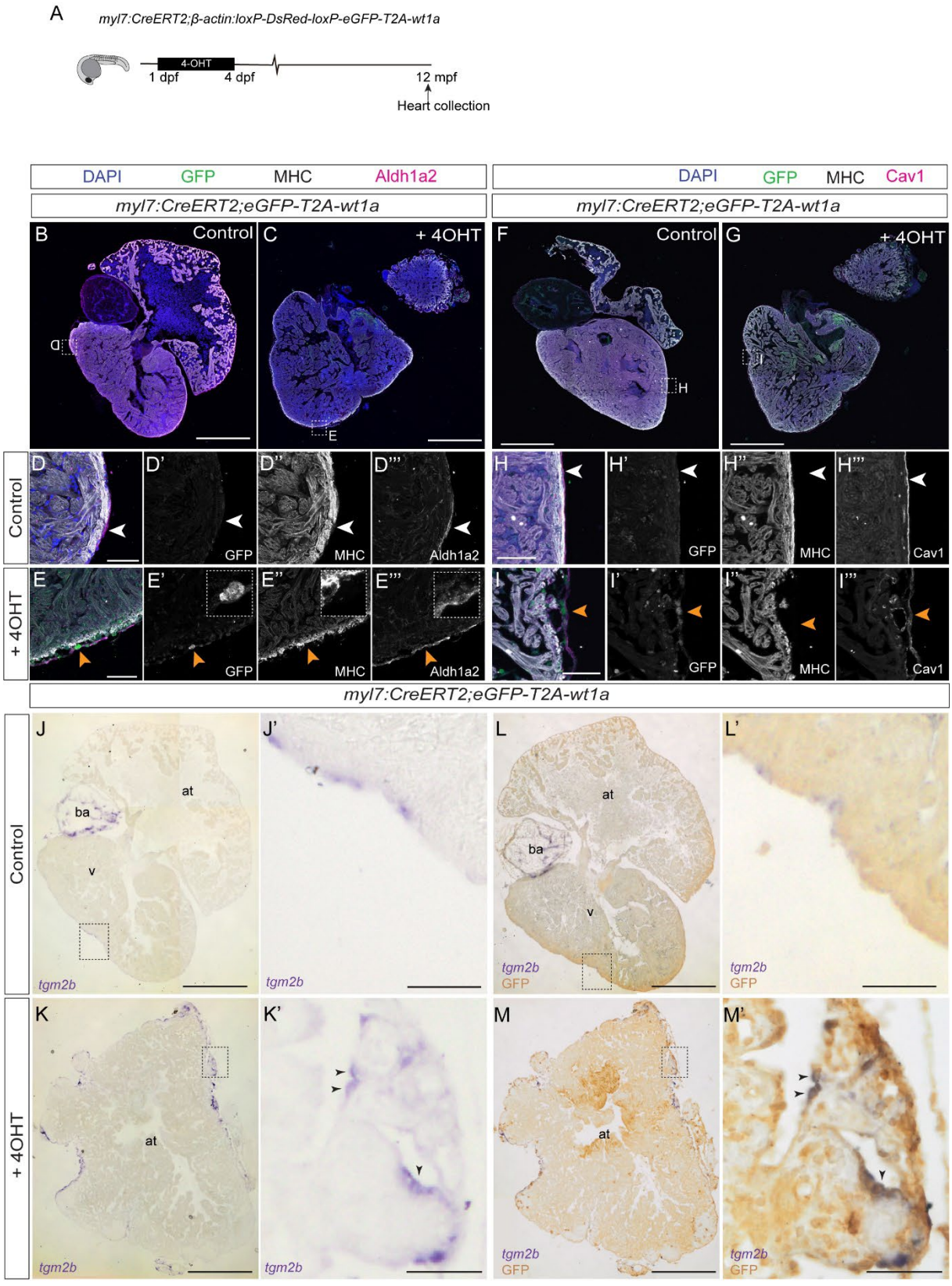

Fig. S4

Fig. S4. *wt1a* overexpression in cardiomyocytes induces expression of epicardial markers in the adult heart.

(A) Schematic representation of the time points during which 4-hydroxytamoxifen (4-OHT) was administered to *myl7:CreERT2;β-actin:loxP-DsRed-loxP-eeGFP-T2A-wt1a* fish (in short *myl7:CreERT2,eeGFP-T2A-wt1a*) and tissue collection.

(B-E’’’) Immunofluorescence against GFP (green), MHC (white) and Aldh1a2 (magenta) on paraffin sections of *myl7:CreERT2;eGFP-T2A-wt1a* and *myl7:CreERT2;eGFP-T2A-wt1a* + 4-OHT adult hearts. Shown are whole heart sections (B,C) and zoomed views in the ventricle (D-E’’’). Zoomed views have been rotated to facilitate comparison between control and overexpression panels. Merged and single channels are shown, as indicated in the panel. White arrowheads, cells positive for Aldh1a2 only. Orange arrowheads point to cells positive for GFP and Aldh1a2 signal that lack MHC staining, and which are located close to the myocardial surface.

(F-I’’’) Immunofluorescence against GFP (green), MHC (white) and Caveolin 1 (Cav1) (magenta) on paraffin sections of *myl7:CreERT2;eGFP-T2A-wt1a* and *myl7:CreERT2;eGFP-T2A-wt1a* + 4-OHT adult hearts. Shown are whole heart sections (F,G) and zoomed views in the ventricle (H,I’’’). Merged and single channels are shown, as indicated in the panel. White arrowheads point to cells positive only for Cav1. Orange arrowheads point to cells positive for GFP and Cav1 signal that lack MHC staining, and which are located close to the myocardial surface.

(J-M’) *in situ* mRNA hybridization against *tgm2b* and immunohistochemistry against eGFP on paraffin sections of *myl7:CreERT2,eeGFP-T2A-wt1a* (J,J’ and L,L’) and *myl7:CreERT2,eeGFP-T2A-wt1a* + 4-OHT (K,K’and M,M’) adult hearts. (J-K’) images of sections after *in situ* mRNA hybridization against the epicardial marker *tgm2b.* (L-M’), same section as in J-K’ after eGFP immunohistochemistry. Black arrowheads in K’ and M’ indicate double positive cells for *tgm2b* and eGFP.

Scale bars: 2000 µm (B, C, F, G, J and L), 50 µm (J’, K’, L’ and M’) and 10 µm (D-E’’’ and H-I’’’) . at, atrium; ba, bulbus arteriosus; Cav1, Caveolin1; MHC, Myosin Heavy Chain; v, ventricle.

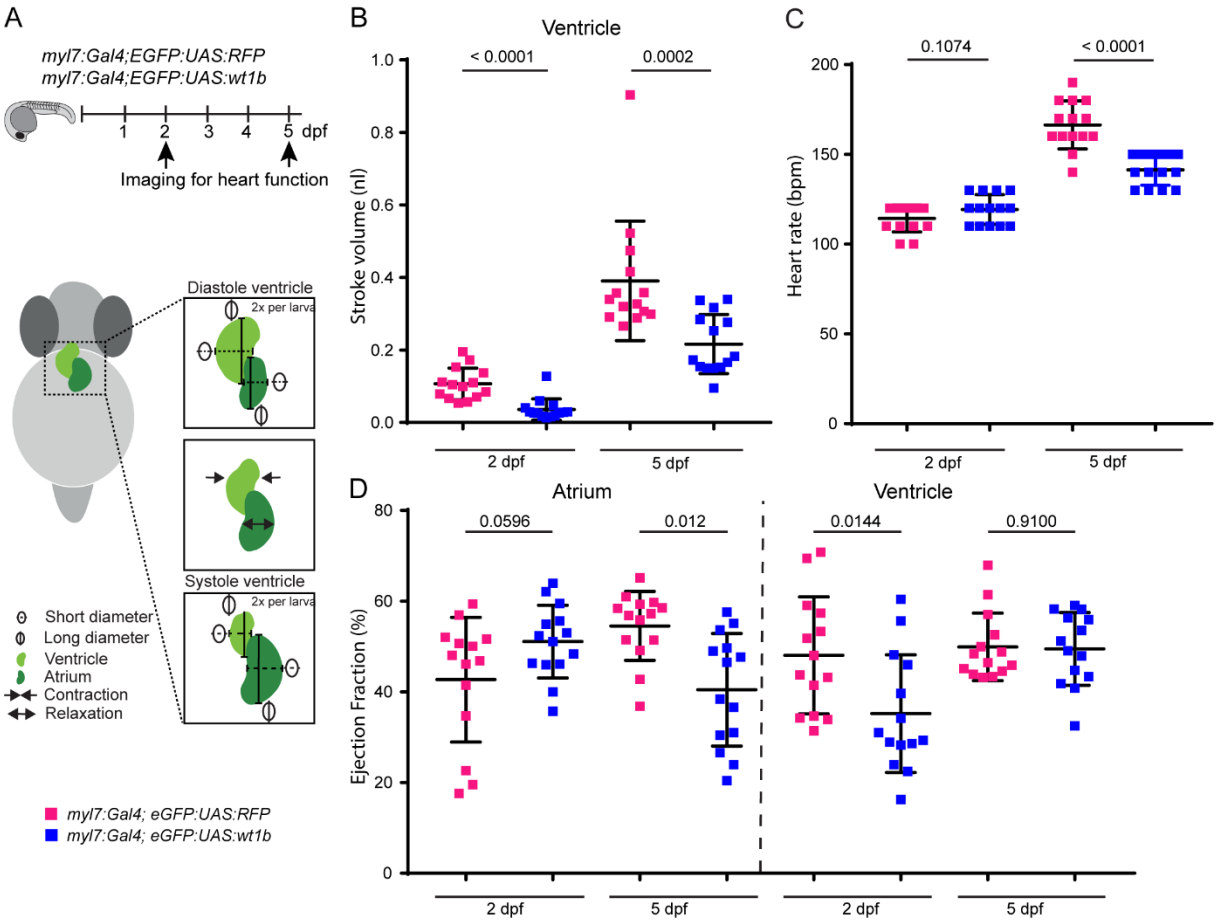

Fig. S5

Fig. S5. Heart function is impaired upon overexpression of *wt1b* in cardiomyocytes.

(A) Schematic representation of the lines used and embryo positioning for image acquisition and the parameters used to determine cardiac function in *myl7:Gal4;eGFP:UAS:RFP* and *myl7:Gal4; eGFP:UAS:wt1b.*

(B) Quantification of ventricular stroke volume at 2 days post fertilization (dpf) and 5 dpf. Statistical significance was calculated with the Mann-Whitney test.

(C) Quantification of the heart rate at 2 dpf and 5 dpf. Statistical significance calculated with an unpaired t-test.

(D) Quantification of ventricular ejection fraction at 2 dpf and 5 dpf. Statistical significance was calculated with an unpaired t-test for the comparison between groups in the atrium and in the ventricle at 2 dpf. Mann-Whitney test was applied to calculate the statistical significance between the groups in the ventricle, at 5 dpf.

In all graphs each point represents one embryo. Shown are also means ±SD.

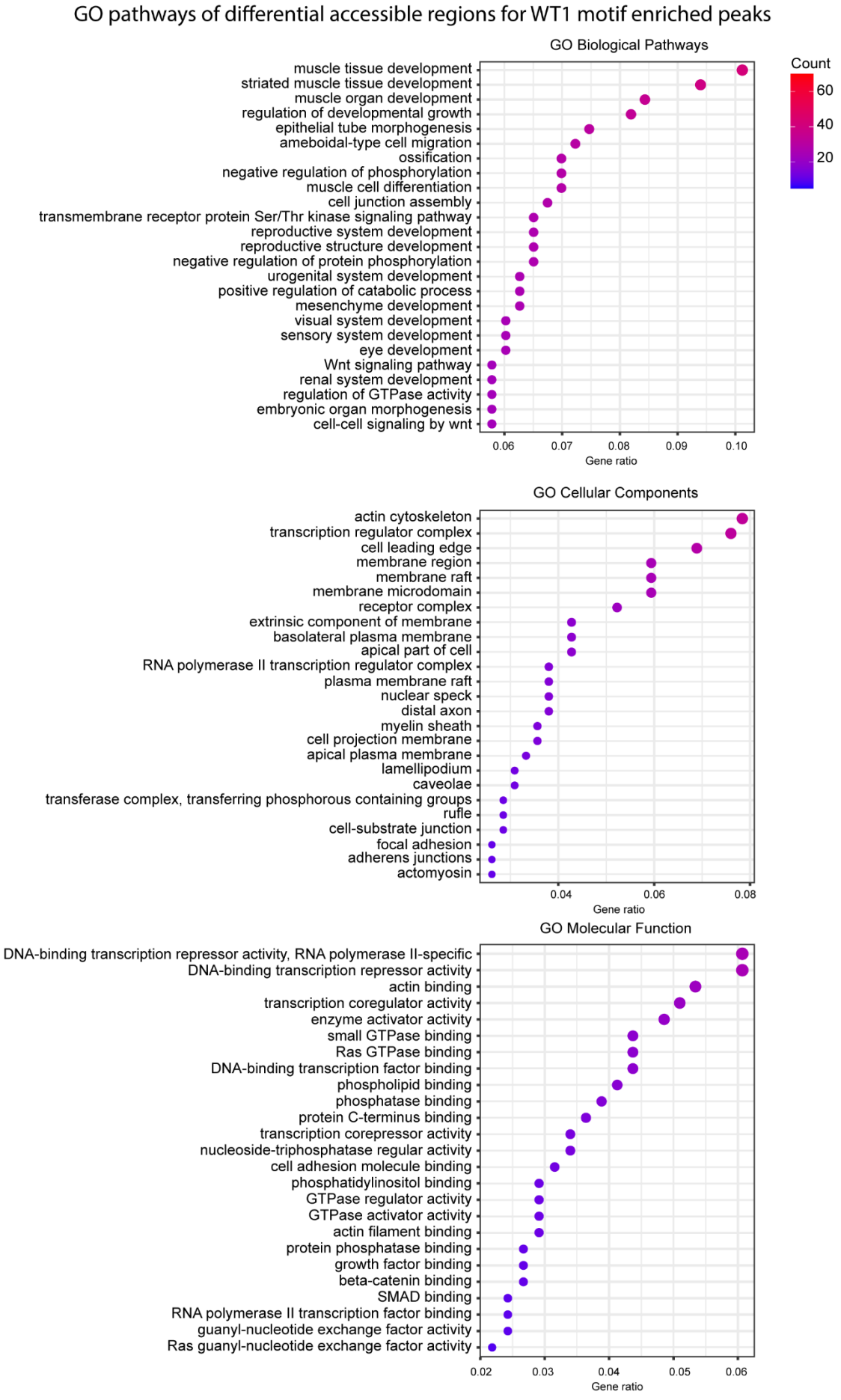
GO pathways of differential accessible regions for WT1 motif enriched peaks
GO Biological Pathways
muscle tissue development
striated muscle tissue development
muscle organ development
regulation of developmental growth
epithelial tube morphogenesis
ameboidal-type cell migration
ossification
negative regulation of phosphorylation
muscle cell differentiation
cell junction assembly
transmembrane receptor protein Ser/Thr kinase signaling pathway
reproductive system development
reproductive structure development
negative regulation of protein phosphorylation
urogenital system development
positive regulation of catabolic process
mesenchyme development
visual system development
sensory system development
eye development
Wnt signaling pathway
renal system development
regulation of GTPase activity
embryonic organ morphogenesis
cell-cell signaling by wnt
0.06
0.07
0.08
0.09
0.10
Gene ratio
Count
60
40
20
GO Cellular Components
actin cytoskeleton
transcription regulator complex
cell leading edge
membrane region
membrane raft
membrane microdomain
receptor complex
extrinsic component of membrane
basolateral plasma membrane
apical part of cell
RNA polymerase II transcription regulator complex
plasma membrane raft
nuclear speck
distal axon
myelin sheath
cell projection membrane
apical plasma membrane
lamellipodium
caveolae
transferase complex, transferring phosphorous containing groups
ruffle
cell-substrate junction
focal adhesion
adherens junctions
actomyosin
0.04
0.06
0.08
Gene ratio
GO Molecular Function
DNA-binding transcription repressor activity, RNA polymerase II-specific
DNA-binding transcription repressor activity
actin binding
transcription coregulator activity
enzyme activator activity
small GTPase binding
Ras GTPase binding
DNA-binding transcription factor binding
phospholipid binding
phosphatase binding
protein C-terminus binding
transcription corepressor activity
nucleoside-triphosphatase regular activity
cell adhesion molecule binding
phosphatidylinositol binding
GTPase regulator activity
GTPase activator activity
actin filament binding
protein phosphatase binding
growth factor binding
beta-catenin binding
SMAD binding
RNA polymerase II transcription factor binding
guanyl-nucleotide exchange factor activity
Ras guanyl-nucleotide exchange factor activity
0.02
0.03
0.04
0.05
0.06
Gene ratio

Fig. S6

Fig. S6. Gene Ontology pathways of differential accessible regions for WT1 motif enriched peaks.

Gene Ontology (GO) pathways enrichment for differential accessible regions that contain the WT1 motif. Shown are the top 25 Biological, Cellular Components and the Molecular Function pathways.

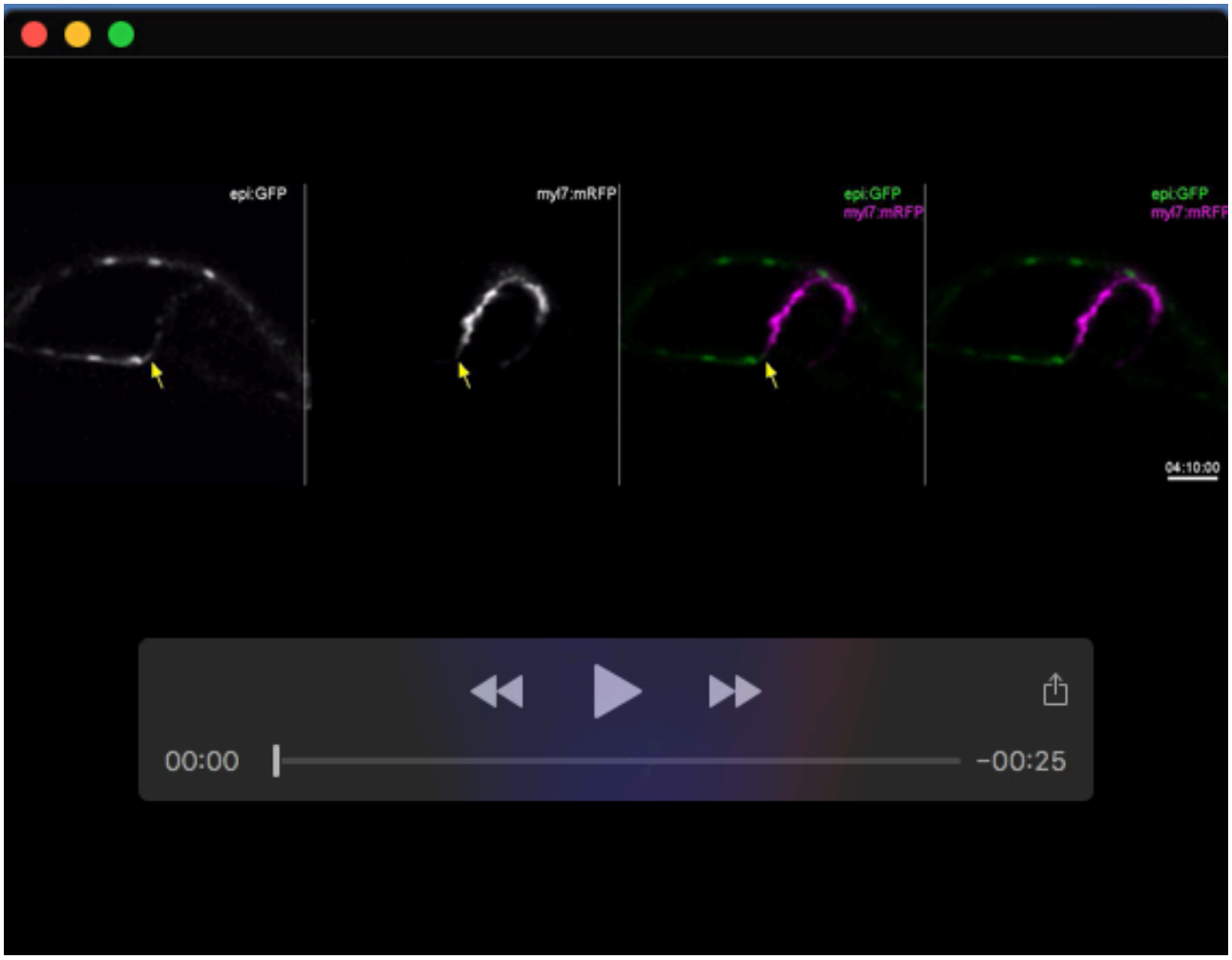

Movie 1. *epi*:eGFP-positive cells at the venous pole switch off GFP expression and start expressing *myl7*:mRFP when entering the heart tube.

In vivo time-lapse imaging of a *epi:GFP;myl7:mRFP* heart between 52 hpf and 68 hpf. The yellow arrow highlights a cell that initially is only GFP positive and latter stops expressing GFP and starts to express RFP. The cyan arrows point to cardiomyocytes in the heart tube that are still GFP-positive at the beginning of the Movie and then loose GFP signal concomitant with increase in mRFP signal intensity. Images were acquired with the Leica TCS SP8 DLS. Shown is a single plane reconstruction of the beating. Scale bar, 50 µm.

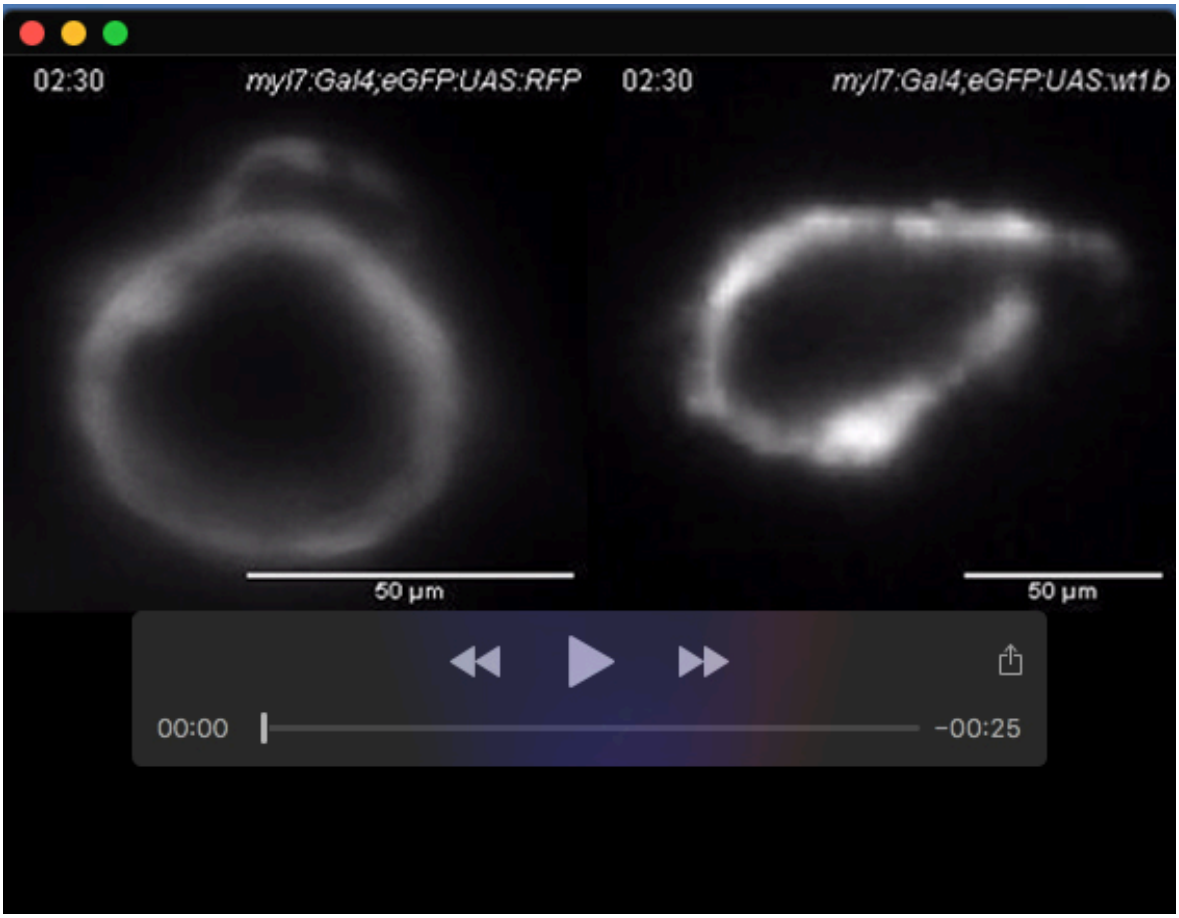

Movie 2. Apical delamination of a *wt1b*-overexpressing cardiomyocyte in a cardiac ventricle at 2 dpf.

In vivo time-lapse imaging of a *myl7:Gal4;eGFP:UAS:RFP* and a *myl7:Gal4;eGFP:UAS:wt1b* heart between 2 and 3 days post fertilization (dpf) acquired with the Leica TCS SP8 DLS confocal microscope, using the digital light sheet (DLS) mode. Shown is the reconstruction of a single plane of the beating ventricle. Note the rounded cells extruding from the ventricle in the *myl7:Gal4;eGFP:UAS:wt1b* heart (right panel, arrow). Scale bar, 50 µm.

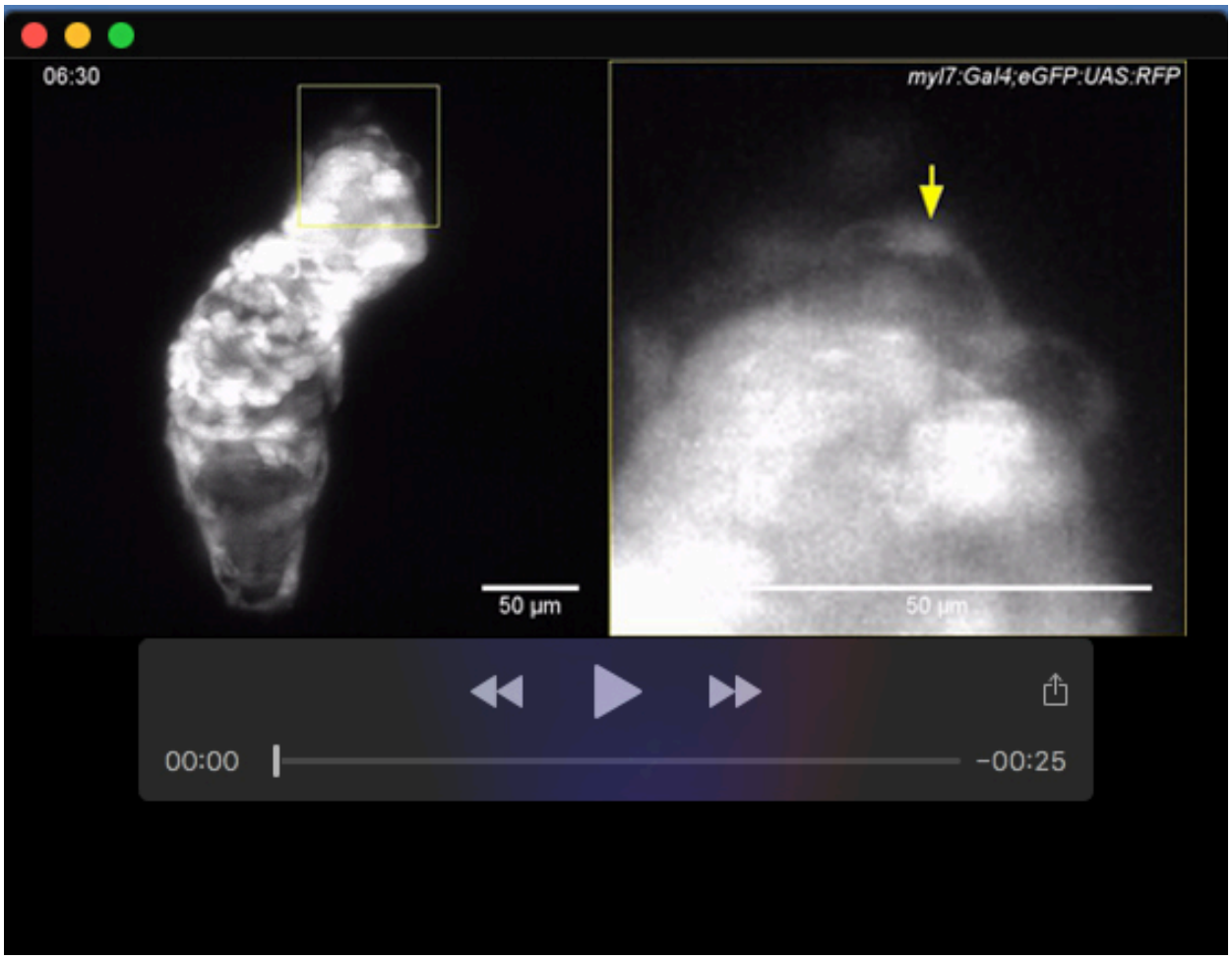

Movie 3. Apical delamination of a *wt1b*-overexpressing cardiomyocyte in a cardiac ventricle at 5 dpf.

In vivo time-lapse imaging of a *myl7:Gal4;eGFP:UAS:wt1b* heart between 5 and 6 days post fertilization (dpf) acquired with the Leica TCS SP8 DLS confocal microscope, using the digital light sheet (DLS) mode. Shown is the reconstruction of a single plane of the beating ventricle. Note how the extruded cells flatten down during the time course of the Movie (Yellow arrow). Scale bar, 50 µm.

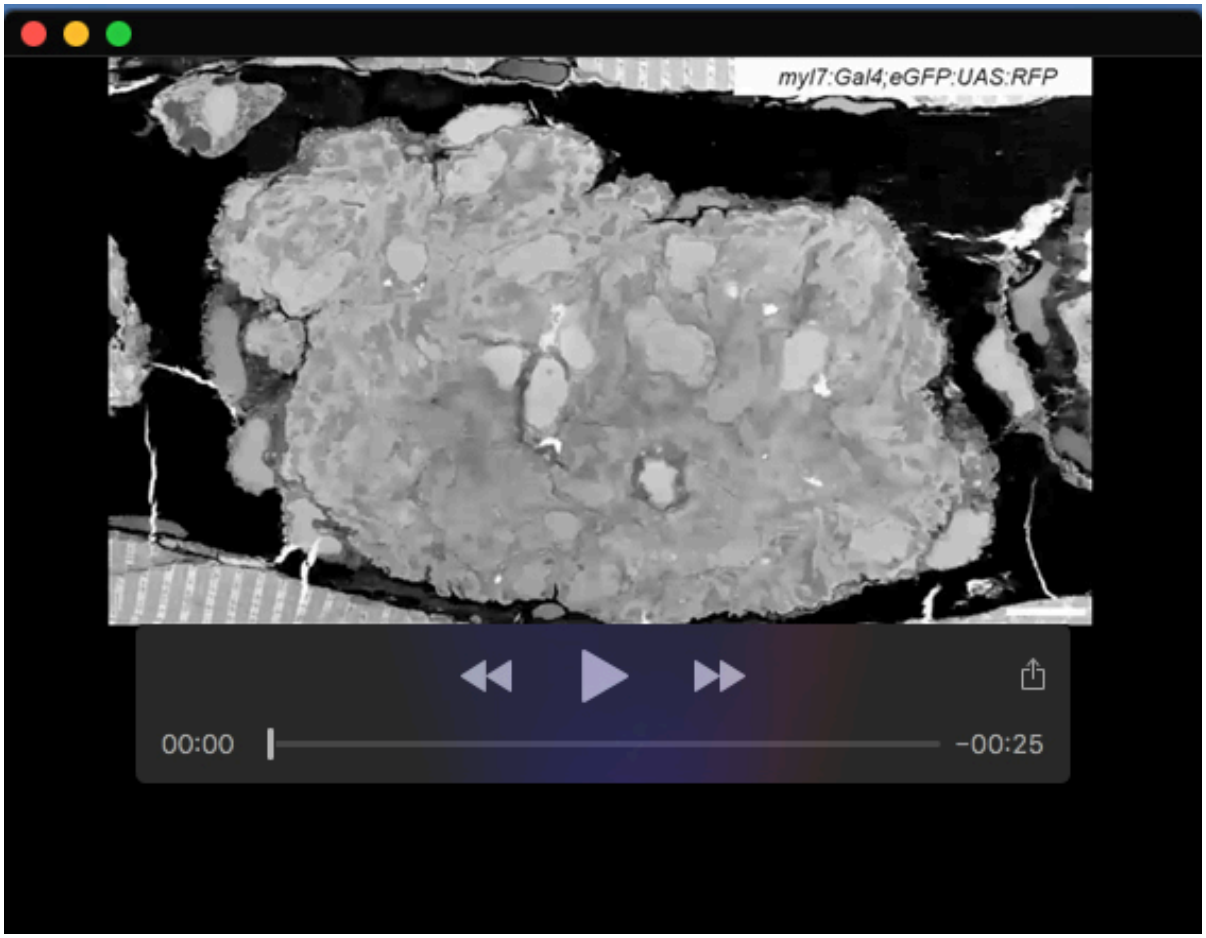

Movie 4. Serial block face scanning z-stacks through a control zebrafish heart at 5 dpf.

Serial stacks through a ventricle from a *myl7:Gal4;eGFP:UAS:RFP* control embryo at 5 dpf. Images were obtained by serial block face scanning electron microscopy. Note the compact organization of the myocardium and the close connection between the myocardium and the endocardium, and how the sarcomeres form a continuous structure between adjacent cardiomyocytes. Of remark is also the dense border between the myocardium and epicardium. EpC, epicardial cell, EnC, endothelial cell, Ery, erythrocyte, CM, cardiomyocyte nuclei. Scale bar 10 µm.

Movie 5. Zoomed view of a serial block face scanning z-stacks through a control zebrafish heart at 5 dpf.

Serial stacks through a ventricle from a *myl7:Gal4;eGFP:UAS:RFP* control embryo at 5 dpf. Images were obtained by serial block face scanning electron microscopy. Shown is a magnification of the myocardium in a region where sarcomeres can be observed. Note the clearly marked z-lines and the longitudinal continuity of the sarcomeres between adjacent cardiomyocytes. Scale bar, 500 nm.

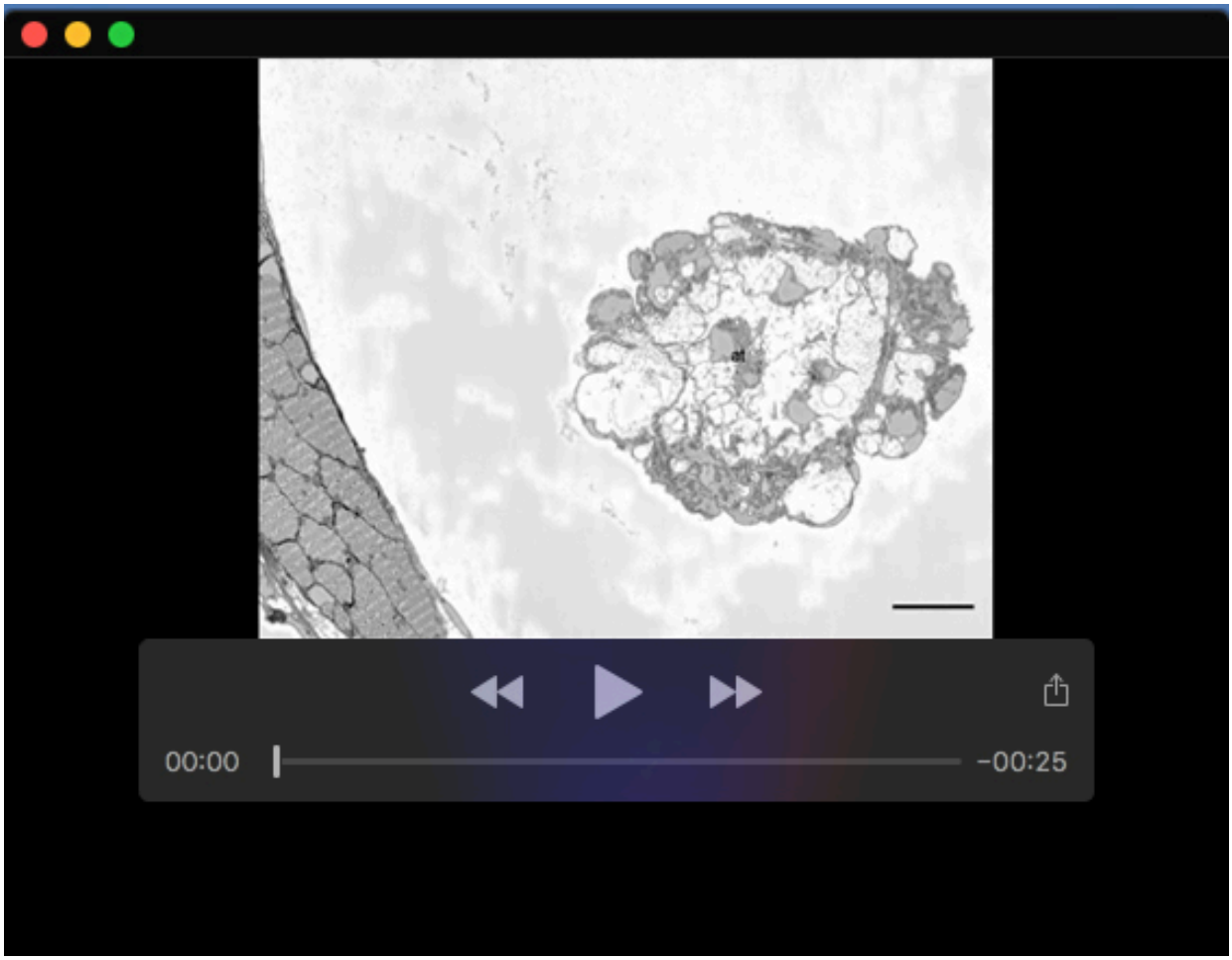

Movie 6. Serial block face scanning z-stacks through a *wt1b*-overexpressing heart at 5 dpf.

Serial stacks through a ventricle from a *myl7:Gal4;eGFP:UAS:wt1b* embryo at 5 dpf. Images were obtained by serial block face scanning electron microscopy. Note the absence of a compact and organized myocardial layer and the enlarged cardiac jelly separating the endocardium and the myocardium. Also visible the extensive areas filled with extracellular matrix. EpC, epicardial cell, EnC, endothelial cell, Ery, erythrocyte, CM, cardiomyocyte, ECM, extracellular matrix, v, ventricle, at, atrium. Scale bar, 20 μm.

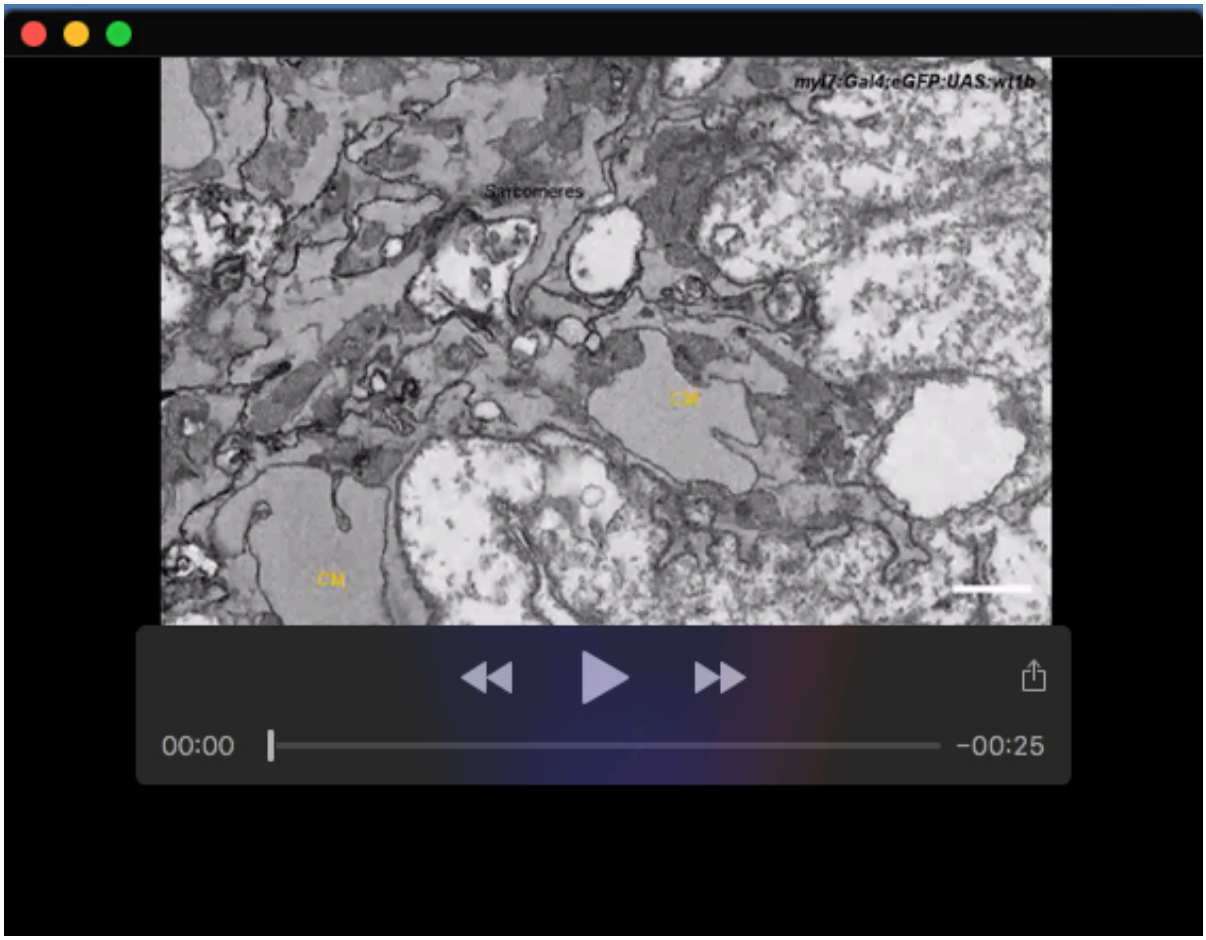

Movie 7. Zoomed view of a serial block face scanning z-stacks through a *wt1b*-overexpressing heart at 5 dpf.

Serial stacks through a ventricle from a *myl7:Gal4;eGFP:UAS:wt1b* embryo at 5 dpf. Images were obtained by serial block face scanning electron microscopy. Shown here is a magnification of the myocardium in a region where sarcomeres can be observed. Note the z-lines. Remarkable is the disorganized arrangement of the sarcomeres between adjacent cardiomyocytes. Scale bar, 500 nm.

Table S1. Differential Peak Calling.

Sheet 1: The file contains about genomic location and information on fold change and significance values of the differential peaks. Columns J-O indicate in which samples peaks were identified (+) or not (-).

Sheet 2: The file contains the same information as sheet 1, with extra information on Peak class, Gene location and direction, zebrafish gene symbol associated with the peak, gene description, mouse ID and whether the gene can also be found on CHIP atlas database for WT1.

Click here to download Table S1

Table S2. Gene Ontology.

Full list of pathways and genes enriched in each of them.

Click here to download Table S2

Table S3. Annotation of differential peaks.

Differential peaks with their associated genes and genomic region classification.

Click here to download Table S3

Table S4. Key resources

REAGENT/RESOURCE	SOURCE	IDENTIFIER
Antibodies		
Rabbit polyclonal anti-Aldh1a2	GeneTex	Cat# GTX124302
Mouse monoclonal anti-CD166 antigen homologue A (neurolin) (Alcama)	DSHB	Cat # ZN-8
Mouse monoclonal anti α-Actinin (sarcomeric) clone EA-53	Sigma Aldrich	Cat # A7811
Mouse monoclonal anti-Caveolin 1	BD biosciences	Cat# 610406
Chicken polyclonal anti-GFP	Aves Labs	Cat# GFP-1010
Mouse monoclonal anti-myosin, sarcomere (MHC)	DSHB	Cat# MF 20, RRID:AB_2147781
Mouse monoclonal anti-ZO-1 (ZO1-1A12)	Invitrogen	Cat # 33-9100
Rabbit anti-Laminin	Sigma Aldrich	Cat # L9393
Mouse monoclonal anti β-Catenin	BD Biosciences	Cat # 610153
Goat anti-Chicken IgY (H+L), Alexa Fluor® 488 conjugate	Thermo Fisher Scientific	Cat # A-11039
Goat anti-Mouse IgG2b, Alexa Fluor® 568 conjugate	Thermo Fisher Scientific	Cat # A-21144
Goat anti-Mouse IgG2b, Alexa Fluor® 647 conjugate	Thermo Fisher Scientific	Cat #A-21242
Goat Anti-Mouse Immunoglobulins/HRP	Dako	Cat # P 0447
Goat anti-Rabbit IgG (H+L) Secondary Antibody, Alexa Fluor® 568 conjugate	Thermo Fisher Scientific	Cat # A-11036
Goat anti-Mouse IgG1, Alexa Fluor® 568 conjugate	Thermo Fisher Scientific	Cat # A-21124
Primers		
Gene	Forward primer	Reverse Primer
Gfp	CAAGATCCGCCACAACATCG	GACTGGGTGCTCAGGTAGTG
wt1a OE	GAGCCATCCCGGAGGTTATG	GGTACTCTCCGCACATCCTG
wt1b OE	CCAGGTCTGACCAGCTGAAG	GTGTCTTCAGGTGGTCCGAG
tcf21	ATGTCCACCGGGTCCATCAG	TCAGGAAGCTGTAGTCCCGCA
Chemicals, Peptides, and Recombinant Proteins		
4-hydroxytamoxifen	Sigma Aldrich	Cat#H6278
N-Phenylthiourea (PTU)	Sigma Aldrich	Cat# P7629
Proteinase K	Roche	Cat# 03115801001
Heparin sodium salt from porcine intestinal mucosa	Sigma- Aldrich	Cat# H4784
Formamide	Sigma- Aldrich	Cat# 47670-1L-F
Blocking reagent	Sigma-Aldrich	Cat# 11096176001
Ribonucleic acid from torula yeast	Sigma- Aldrich	Cat# R6625-25G
HBSS (10X), no calcium, no magnesium, no phenol red	Thermo Fisher Scientific	Cat# 14185052
Corning™ 0.05%	Thermo Fisher Scientific	Cat# MT25051CI

REAGENT/RESOURCE	SOURCE	IDENTIFIER
Trypsin/0.53 mM EDTA in HBSS w/o Calcium and Magnesium		
Collagenase	Sigma	Cat # C8176
BSA	Sigma	Cat# A3059
Kits		
SMARTer® Ultra™ Low Input RNA for Illumina® Sequencing – HV kit	Takara	Cat# 634828
Agilent's High Sensitivity DNA Kit	Agilent	Cat# 5067-4626
Low Input Library Prep Kit	Illumina	Cat# 634947
Illumina Nextera kit	Illumina	Cat# Fc-121-1030
Illumina Tagment DNA TDE1 Enzyme and Buffer Kits	Illumina	Cat# 20034198
DT® for Illumina Nextera DNA Unique Dual Indexes Set C	Illumina	Cat# 20027215
Bioline MyFi Mix	Meridian Bioscience	Cat# Bio-25050
MinElute PCR Purification Kit	Qiagen	Cat# 28004
AMPure XP	Beckman Coulter	Cat # A63882
Qubit dsDNA HS Assay Kit	Thermo Fisher Scientific	Cat# Q32854
NGS Fragment Kit	Agilent	Cat# DNf-473
Bioline JetSeq library Quantification Lo-ROX kit	Meridian Bioscience	Cat# Bio-68029
NovaSeq XP 2-Lane Kit v1.5	Illumina	Cat# 20043130
NovaSeq 6000 SP Reagent Kit v1.5	Illumina	Cat# 20040719
Software and Algorithms		
Fiji	NIH	SCR_002285
GraphPad Prism 7	GraphPad Software	SCR_002798
Imaris 9.5.1	Bitplane	
MATLAB R2017a	MathWorks	
Specialized Material		
U-shaped glass capillaries	Leica microsystems	Cat # 158007061
MatTek imaging dish, 35 mm	MatTek Corporation	Cat # P35G-0-20-C
Tungsten needles		
Microscopes and Imaging machines		
Nikon SMZ800N	Nikon	
Leica TCS SP8 digital light sheet (DLS)	Leica	
Imager M2	Zeiss	
LSM 880 confocal microscope, with Airyscan	Zeiss	
Quanta FEG 250 SEM (serial block face scanning electron microscope)	FEI	
Experimental Models: Organisms/Strains		
Et(-26.5Hsa.WT1-gata2:eGFP)^{cn1} (epi:eGFP)	(Peralta et al., 2013)	ZDB-ETCONSTRCT-170823-1

REAGENT/RESOURCE	SOURCE	IDENTIFIER
Tg(myl7:mRFP)^{ko08Tg}	(Rohr et al., 2008)	ZDB-TGCONSTRCT-080917-1
Tg(fli1a:Gal4)^{ubs3Tg}	(Herwig et al., 2011)	ZDB-ALT-120113-6
Tg(myl7:Gal4)^{cbg2Tg}	(Mickoleit et al., 2014)	ZDB-TGCONSTRCT-150108-1
Tg(–3.5ubi:loxP-eGFP-loxP-mCherry)^{cz1701}	(Mosimann et al., 2011)	ZDB-TGCONSTRCT-110124-1
Tg(eGFP:5xUAS:RFP; gcryst:cerulean)^{cn15}	(Sanz-Morejon et al., 2019)	ZDB-TGCONSTRCT-190724-4
Tg(wt1a:CreERT2); ^{cn10Tg}	(Sánchez-Iranzo et al., 2018)	ZDB-TGCONSTRCT-170711-9
Tg(-3.5ubi:loxP-EGFP-loxP-mCherry) ^{cz1701Tg}	(Mosimann et al., 2011)	ZDB-ALT-110124-1
Tg(bGI-eGFP:5xUAS:wt1b -bGI; cryaa:eCFP)^{brn4}	This manuscript	ZDB-ALT-200327-14
Tg(bactin2:loxP-DsRed2-loxP-eGFP-T2A-wt1a)^{li21}	This manuscript	N/A
Tg(bGI-eGFP:5xUAS:tcf21 -bGI; cryaa:eCFP)^{brn5}	This manuscript	N/A